Equilibrium structure and off-equilibrium kinetics of a magnet with tunable frustration

Federico Corberi
Dipartimento di Fisica "E.R. Caianiello", and INFN, Gruppo Collegato di Salerno, and CNISM, Unità di Salerno, Università di Salerno, via Giovanni Paolo II 132, 84084 Fisciano (SA), Italy

Manoj Kumar and Sanjay Puri
School of Physical Sciences, Jawaharlal Nehru University, New Delhi 110067, India

Eugenio Lippiello
Dipartimento di Matematica e Fisica, University of Campania "L. Vanvitelli", viale Lincoln, 5 81100 Caserta, Italy
(Received 12 April 2017; published 29 June 2017)

We study numerically a two-dimensional random-bond Ising model where frustration can be tuned by varying the fraction a of antiferromagnetic coupling constants. At low temperatures the model exhibits a phase with ferromagnetic order for sufficiently small values of a, $a < a_f$. In an intermediate range, $a_f < a < a_a$, the system is paramagnetic, with spin-glass order expected right at zero temperature. For even larger values, $a > a_a$, an antiferromagnetic phase exists. After a deep quench from high temperatures, slow evolution is observed for any value of a. We show that different amounts of frustration, tuned by a, affect the dynamical properties in a highly nontrivial way. In particular, the kinetics is logarithmically slow in phases with ferromagnetic or antiferromagnetic order, whereas evolution is faster, i.e., algebraic, when spin-glass order is prevailing. An interpretation is given in terms of the different nature of phase space.

DOI: 10.1103/PhysRevE.95.062136

I. INTRODUCTION

When a system is brought across a phase-transition toward a state where the initial symmetry is spontaneously broken, a slow nonequilibrium evolution sets in. A paradigm is represented by binary systems [1], such as ferromagnets, cooled from above to below the critical temperature T_c. In the clean case, namely in the absence of any kind of quenched disorder or inhomogeneities, the kinetics is characterized by a coarsening process that is nowadays quite well understood. Domains of the symmetry-related equilibrium phases at the final temperature T_f form and their typical size $L(t)$ grows in time. This process is endowed with a scaling symmetry such that configurations visited at different times are statistically equivalent provided lengths are measured in units of $L(t)$. The growth law of the domains' size is generally algebraic $L(t) \sim t^{1/z}$. The dynamical exponent z is temperature independent and varies only among different dynamical universality classes which—in turn—are determined by the symmetry of the order parameter, i.e., if scalar or vectorial, and by the character of the dynamics, e.g., in the presence of conservation laws, hydrodynamics, etc.

Phase-ordering can occur in disordered ferromagnets as well. In these systems an amount of quenched randomness is present, but its effects are sufficiently weak not to spoil the basic structure of the equilibrium state. A disordered phase at high temperature and a low temperature one are still present and the symmetry breaking mechanism is akin to that of clean magnets—e.g., up-down (or Z_2) symmetry is spontaneously broken for a scalar order parameter. Examples are magnetic models in the presence of random external fields, coupling constants with a stochastic component, or quenched vacancies [2].

If disorder is sufficiently weak not to change the equilibrium structure, its presence is by far much more important as dynamical properties are concerned. Indeed, one observes that even the smallest amount of randomness usually slows down dramatically the asymptotic growth law of the domains. This is because quenched disorder pins the dynamics introducing energetic barriers, which can only be exceeded by rare thermal fluctuations. Therefore, at variance with the clean systems, the dynamical features are strongly temperature dependent.

While equilibrium properties are sometimes quite understood, thanks also to some general results such as the Harris criterion, understanding of the off-equilibrium evolution is by far incomplete. Concerning the growth law of the domains' size, either logarithmic or temperature-dependent power laws have been reported both in experiments [3–6] and in model systems [7–28], and there is yet no clear indication of a simple classification—e.g., on the basis of some dynamical universality classes—of the behavior of different disordered magnets. Moreover, despite the fact that disorder is responsible for pinning and slowing down of the kinetics, the simple idea that the more disorder is present in a system the slower the evolution will be, has been recently shown [24–26] to be incorrect in quite a number of cases. Considering, for instance, the Ising model with random dilution (namely a fraction d of sites or bonds on the lattice are missing), it was shown that, although for sufficiently small values of d, the kinetics is slowed down upon increasing d, as naively expected, after a certain threshold increasing d produces a faster growth. As it is explained in Refs. [24,25], this happens because adding more disorder—in this case parametrized by d—not only one introduces more pinning sources but, more importantly, the topological properties of the system are also changed. Indeed, when d gets close to the value d_c, where the set of nondiluted sites (or bonds) is at the percolation threshold, the fractal properties of the network play an important role in speeding up the evolution, because the pinning barriers are softened.

This very effect, the nonmonotonous behavior of the speed of growth versus the amount of disorder, is observed not only in diluted systems but also for Ising spins with random

ferromagnetic couplings [24], the kind of model that will be generalized with the addition of frustration in this article.

All the systems described insofar are nonfrustrated. When it is impossible to simultaneously satisfy all the interactions between the microscopic constituents, as in the paradigmatic example of the antiferromagnetic Ising model on the triangular lattice, frustration arises. The slow evolution of disordered frustrated systems is by far a much more complicated problem. This is because even the basic structure of the low-temperature equilibrium states in finite-dimensional systems is still debated. The absence of a clear-cut indication on the static properties hinders the interpretation of what is dynamically observed. Indeed, in a droplet theory scenario, one would expect a kind of coarsening reminiscent of what was previously discussed for ferromagnetic systems, while if a picture inspired to the mean-field solution applies, something very different should happen [29].

The aim of this paper is to gradually near the study of the kinetics of disordered systems with frustration from the side of nonfrustrated ones, where a better understanding has been to some extent achieved. In order to do that we consider an Ising model with a fraction a of antiferromagnetic coupling constants, and the remaining ones are ferromagnetic. We study the model numerically in two dimensions as the value of a is varied in $[0,1]$. Clearly, by changing the parameter a, one can gradually tune the amount of frustration present in the system. Not enough, in order to soften as possible the crossover from a situation without frustration to one where it is relevant, we consider the case where the ferromagnetic interactions are much stronger than the antiferromagnetic ones. This allows us to stay as close as possible—so to say—to the simpler and better understood ferromagnetic situation.

In the low-temperature equilibrium phase-diagram of the model, as a is progressively increased, one moves from a ferromagnetic phase, where frustration plays a minor role, to a strongly frustrated paramagnetic phase which, right at $T = 0$, is expected [30] to exhibit spin glass order [31]. For even larger values of a, an antiferromagnetic region is entered. Therefore, considering the evolution of the present model after a deep quench to a small finite temperature $T_f > 0$, one has the opportunity to study how different amounts of frustration influence the off-equilibrium kinetics. In doing that we find that in the magnetic phases—either ferromagnetic or antiferromagnetic—a usual coarsening is observed characterized by a logarithmic increase of the domains' size $L(t)$, in agreement with previous studies on related Ising models with random bonds [32]. Upon increasing frustration, the speed of phase-ordering changes in a nonmonotonous way. This behavior, which is analogous to the one discussed above for nonfrustrated systems, can be interpreted along similar arguments based on topology. Indeed, the geometry of the growing domains becomes fractal as a is increased and the transition to the paramagnetic region is approached, similar to what happens in the nonfrustrated diluted systems previously considered when the percolation threshold is approached. Also in this case, the fractal topology speeds up the evolution.

This shows that an off-equilibrium evolution getting faster and more efficient with the addition of disorder is of a quite general nature and occurs both in systems with and without frustration. At variance with the logarithmically slow evolution observed in the ferro- or antiferromagnetic phases, a faster kinetics characterized by algebraic behaviors is found along the whole paramagnetic region, where frustration plays a prominent role. In this region, although neither ferromagnetic, antiferromagnetic, or spin-glass order [31] are present at finite temperatures, a quench to $T_f > 0$ exhibits slow evolution as due to the proximity of the spin-glass ground state at $T_f = 0$ [30]. Due to that, the faster evolution observed in this phase (as compared to the logarithmic one in the ferro- and antiferromagnetic regions) can be perhaps ascribed to the spin glass structure with many quasi isoenergetic levels and softer barriers as opposed to those present in a ferromagnetic phase with two profound free energy minima.

This paper is organized as follows: In Sec. II, we introduce the model, set the notation, and discuss the structure of the bond network in Sec. II A. Section III is devoted to the study of the low-temperature phase-diagram of the system. The results concerning the kinetics of the model after deep quenches to various final temperatures are presented and discussed in Sec. IV. Finally, we summarize and draw our conclusions in the last Sec. V.

II. THE MODEL

We consider the Ising model with Hamiltonian

$$\mathcal{H}(\{s_i\}) = -\sum_{\langle ij\rangle} J_{ij} s_i s_j, \tag{1}$$

where the $s_i = \pm 1$ are spin variables, the sum runs over nearest-neighbors couples $\langle ij\rangle$ of a lattice, and the coupling constants are $J_{ij} = J_0 + \xi_{ij}$, where $J_0 > 0$ and the ξ_{ij} are uncorrelated random variables extracted from a bimodal distribution,

$$P(\xi) = a\,\delta_{\xi,-K} + (1-a)\,\delta_{\xi,K}, \tag{2}$$

where δ is the Kronecker function and $0 \leqslant a \leqslant 1$ and K are parameters. In a previous paper [24], we studied the kinetics of this model without frustration, with $K < J_0$, namely with only ferromagnetic interactions. Here, instead, we set

$$K > J_0, \tag{3}$$

meaning that the fraction a of bonds with $\xi_{ij} < 0$ are antiferromagnetic and the remaining ones are ferromagnetic. We will also denote with $J_- = J_0 - K$ and $J_+ = J_0 + K$ the strength of such bonds, respectively. We will consider a square lattice in $d = 2$ with periodic boundary conditions.

Next to the ferromagnetic local order parameter s_i, the spin, it is useful to introduce the antiferromagnetic one,

$$\sigma_i = (-1)^i s_i, \tag{4}$$

or *staggered* spin. In Eq. (4) it is stipulated that the index i runs over the lattice sites in such a way that two nearest neighbors always have an opposite value of $(-1)^i$.

A classification of the low-temperature equilibrium states will be made in Sec. III in terms of their spontaneous magnetization,

$$m = \frac{1}{N}\sum_i s_i, \tag{5}$$

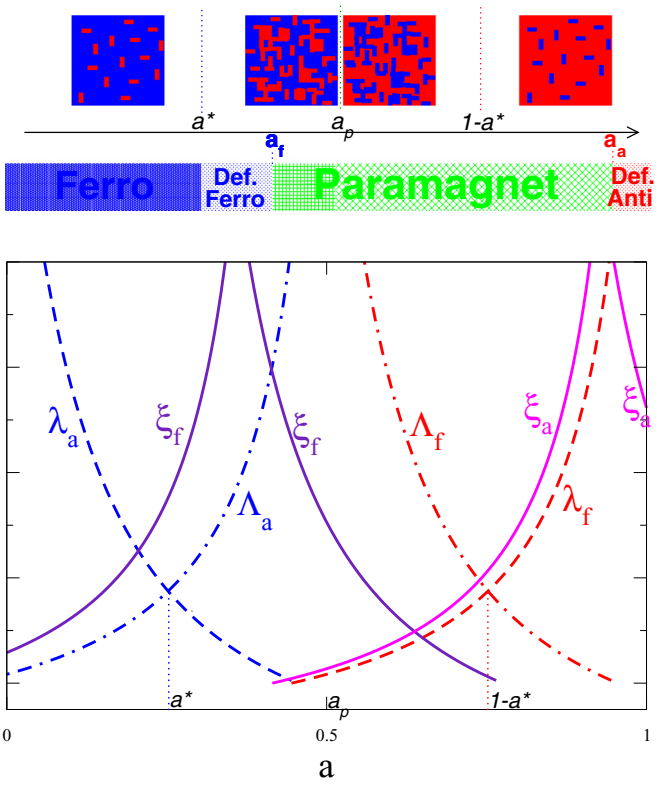

FIG. 1. In the upper stripe, four typical bond configurations are pictorially shown, corresponding to $0 < a < a^*$, $a^* < a \lesssim a_p$, $a_p \lesssim a < 1 - a^*$, and $1 - a^* < a < 1$, from left to right, respectively. Ferromagnetic bonds are drawn in blue, antiferromagnetic ones in red. The bar below the configuration stripe describes the physical phases of the systems as a is varied, e.g., if ferromagnetic, paramagnetic, etc. The graph in the lower part of the figure is a schematic representation of the behavior of the typical lengths characterizing the bond configuration and the physical properties (see text).

and of the staggered magnetization,

$$M = \frac{1}{N}\sum_i \sigma_i. \tag{6}$$

A. The geometry of the bond network

It is useful to discuss the geometrical properties of the network of bonds of the model, which is pictorially illustrated in the upper stripe of Fig. 1. With $a = 0$ the system is the usual clean Ising ferromagnet, since all the coupling constants are positive. Moving to a finite a amounts to adding some antiferromagnetic bonds. If a is small, these will be separated apart by a typical distance,

$$\lambda_a \sim a^{-1/d}. \tag{7}$$

This situation is schematically represented in the leftmost box on the upper stripe of the figure. Here the blue color corresponds to regions where the bonds are ferromagnetic, while antiferromagnetic ones are drawn in red. The behavior of λ_a is shown by a dashed blue line in the lower graph of Fig. 1. It decreases as a raises, meaning that at some point it becomes of the order of the lattice spacing and groups of antiferromagnetic bonds start to coalesce. Indeed, we know that for $a = a_p = 1/2$ such bonds form a percolating cluster, since the bond percolation threshold is precisely a_p. Due to this, right at a_p the size Λ_a of the regions of clustered antiferromagnetic bonds is $\Lambda_a = \infty$ and, for a smaller but not to far from $a = a_p$ one has the well-known percolative behavior,

$$\Lambda_a = (a_p - a)^{-\nu}, \tag{8}$$

with $\nu = 4/3$, which is shown by a dotted-dashed blue line in the lower part of Fig. 1. A pictorial representation of the bond configuration in the region $a \lesssim a_p$ is shown in the second (from the left) box in the upper part of the figure. The transition between the region with isolated and clustered antiferromagnetic bonds occur at a value $a = a^*$, which can be roughly identified as the point where $\lambda_a \simeq \Lambda_a$. The actual value of a^* is located [24] between $a = 0.2$ and $a = 0.3$.

Clearly, as we move in the region $a > a_p$ the situation mirrors that for $a < a_p$ upon exchanging the roles of ferromagnetic and antiferromagnetic bonds and substituting the lengths λ_a, Λ_a with the corresponding ones λ_f, Λ_f relative to the ferromagnetic bonds, for which one has

$$\lambda_f = (1 - a)^{-1/d}, \tag{9}$$

and

$$\Lambda_f = (a - a_p)^{-\nu}. \tag{10}$$

III. THE STRUCTURE OF THE EQUILIBRIUM STATES

When $J_0 > 0$ the symmetry of the bond geometry for $a < a_p$ and $a > a_p$ is spoiled because the actual absolute value of positive and negative bonds is different. Furthermore, the simultaneous presence of positive and negative couplings may introduce frustration and make the system highly nontrivial as in the notable case of a spin glass, which can be obtained in the present model by letting $J_0 = 0$. In this paper, we focus on the somewhat simpler case, with

$$K < \frac{z}{z-2} J_0, \tag{11}$$

where z is the coordination number of the lattice. Equation (11) is a *ferromagnetic-always-wins* condition. Indeed, it can be simply checked that, when Eq. (11) holds, a spin to which at least a ferromagnetic bond is attached will always lower its energy by pointing along the direction of the majority (if a majority exists) of spins to which it is connected by ferromagnetic bonds. For instance, a spin attached to a single ferromagnetic bond will decrease its energy by aligning with the spin on the other side of that bond, irrespective of the configuration of the other $z - 1$ neighboring spins. Still being frustrated, a system conforming to the condition Eq. (11) has a simpler structure—although not trivial at all—of the low-temperature equilibrium states, as we will see shortly. Notice also that the spin glass do not obey Eq. (11) (since $J_0 = 0$). All the numerical data that will be presented in the following refer to the case $J_0 = 1$, $K = 5/4$, which obviously obeys Eq. (11).

Let us now discuss the structure of the low-temperature equilibrium states of the model as a is changed.

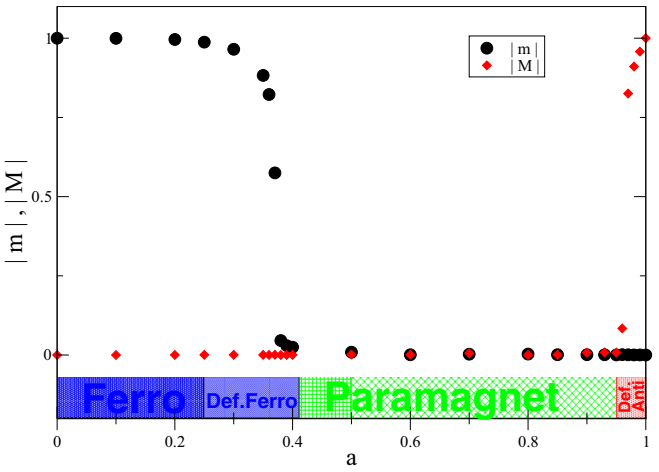

FIG. 2. $|m|$ and $|M|$ at $T = 0$ for different values of a.

A. Ground states

In the following, we will focus on the ground states, namely the equilibrium configurations at $T = 0$. We found these states by a generalization [33] to systems with periodic boundary conditions of the algorithm introduced in Ref. [34]. With this technique the ground state can be found in polynomial time. We will postpone the discussion of the effects of a finite temperature to Sec. III B.

The global order parameters m and M defined above, computed in the ground states of the model for different values of a, are shown in Fig. 2. We will classify the ground states according to m and M in the different regions of the parameter a in the following sections. This classification is reported in the upper bar of Fig. 1 and, similarly, in the lower bar of Fig. 2.

1. *Ferromagnetic* ($0 \leqslant a < a_f$)

Let us start discussing the ferromagnetic phase, which can be split in the two sectors with $0 \leqslant a < a^*$ and $a^* \leqslant a < a_f$, which will be considered separately below.

Sector $0 < a < a^*$

As discussed above in Sec. II A, in this region there are basically only isolated antiferromagnetic links in a sea of ferromagnetic ones. At $T = 0$ spins in this sea necessarily align in a ferromagnetic state. Condition Eq. (11) implies that also the spins attached to the antiferromagnetic bonds must be aligned with those in the sea. Hence, the ground state is akin to a usual ferromagnetic system. Of course, as a increases, there is a finite probability to find some antiferromagnetic bonds nearby and this can cause some spin reversal with respect to a completely ordered configuration, but for $a < a^*$ these are quite few. Since the presence of antiferromagnetic bonds is largely irrelevant in this parameter region, we expect $|m| \simeq 1$ and $M = 0$. We see in Fig. 2 that this is indeed the case.

A representation of a real ground state for $a = 0.2 < a^*$ (let us recall that a^* is expected to be located between $a = 0.2$ and $a = 0.3$) is shown in the upper left panel of Fig. 3, which confirms the description above.

Sector $a^* \leqslant a < a_f$

Figure 2 shows that ferromagnetic order extends up to a certain $a = a_f$ (with $a_f \gtrsim 0.4$), which is well beyond a^*. Ferromagnetic ordering occurring beyond a^* does not come as a surprise, since in the whole region $a < a_p$ the number of ferromagnetic bonds is larger than that of the

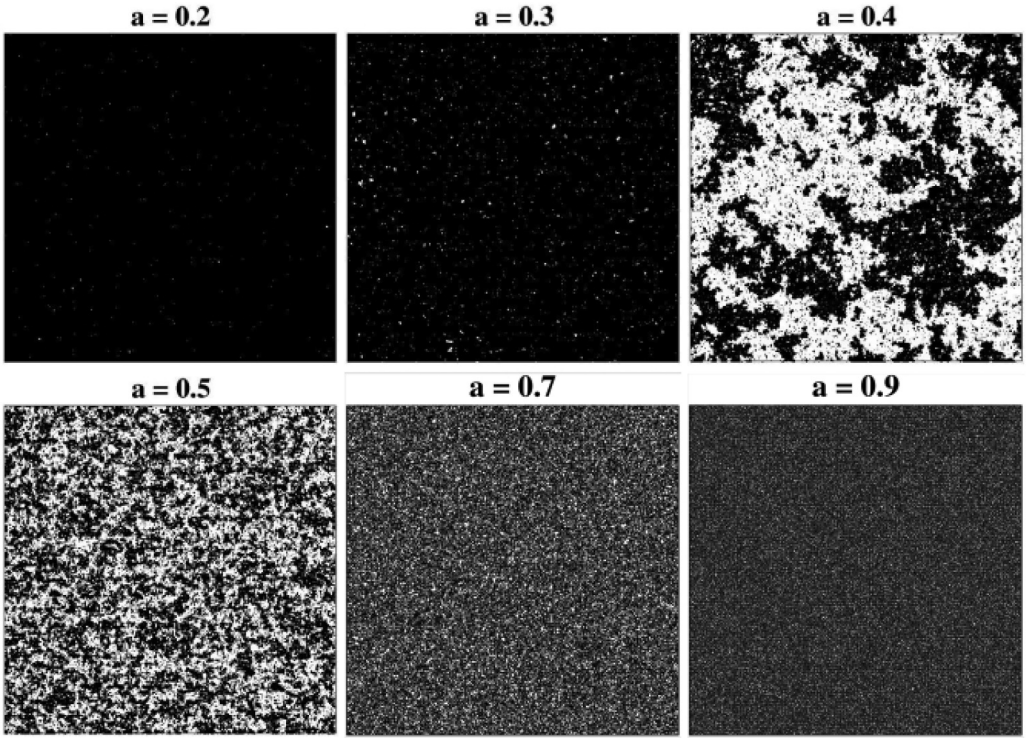

FIG. 3. Configurations of the ground state for a system of size $\mathcal{L} = 512$ for different values of a. Spins up are plotted in black, spins down in white.

antiferromagnetic ones and also because of the *ferromagnetic-always-wins* condition Eq. (11). Notice, however, that this does not guarantee that ferromagnetic order is sustained up to $a = a_p$ or beyond, for the reasons that will be explained in Sec. III A 2, but only up to a lower value $a = a_f < a_p$.

In the region $a^* < a < a_f$ there is still a prevalence of ferromagnetic order, namely the fraction of—say—up spins prevails over the reversed ones, but since antiferromagnetic bonds can coalesce, regions with down spins may be found locally, as it can be seen in Fig. 3 for $a = 0.3$ and $a = 0.4$ (upper central and right panel). This is why we call this situation *defective ferromagnet*. Clearly, the islands where spins are reversed increase upon raising a, as it can be checked in Fig. 3. Here one sees that the size ξ_f of these regions grows dramatically as a gets close to a_f, a fact that is pictorially sketched in Fig. 1, as in the presence of a continuous phase-transition. The presence of extended regions opposite to the dominant order clearly depletes the magnetization of the system, so when $a < a^* < a_f$ one has $0 < |m| < 1$ (decreasing upon raising a) and $M = 0$, as it can be observed in Fig. 2. The magnetization m vanishes at the transition point $a = a_f$.

2. *Paramagnetic phase ($a_f \leqslant a \leqslant a_a$)*

We discuss separately the two subregions with $a_f < a < a_p$ and $a_p < a < a_a$ below.

Sector $a_f < a < a_p$

Here the ferromagnetic bonds still prevail and form a sea that spans the system. The difference with the ferromagnetic region is that antiferromagnetic bonds, besides being grouped together, can form sufficiently connected paths as to destroy the ferromagnetic state. This is discussed in Appendix A.

A real configuration of the system in this region looks like the one for $a = 0.5$ in Fig. 3 (bottom raw, left). Notice also that, upon comparing this configuration with the one at $a = 0.7$, one sees that the size ξ_f of the locally magnetized regions increases as a decreases toward a_f, suggesting that ξ_f diverges also on this side of a_f, as it is sketched in Fig. 1.

Given the structure of the ground state discussed above, one has $m = 0$. Clearly, it is also $M = 0$, since negative bonds are a minority and there cannot be antiferromagnetic ordering. This is confirmed in Fig. 2. For this reason we generically denote the region with $a_f \leqslant a \leqslant a_a$ as *paramagnetic*. Let us anticipate, however, that right at $T = 0$ some spin-glass order is expected, as we will further discuss in Sec. IV A 2.

Sector $a_p < a < a_a$

In this region there is a sea of antiferromagnetic bonds. If a is larger but sufficiently close to a_p there are also ferromagnetic islands inside which spins are aligned. However, these islands are disconnected and hence they order incoherently. Therefore, we expect $m = 0$ throughout the region $a > a_p$. This is observed in Fig. 2. The presence of a spanning sea of antiferromagnetic bonds is not sufficient to guarantee that a global antiferromagnetic order will establish, not even if a is so large that ferromagnetic bonds are isolated, which happens for $a > 1 - a^*$ (we recall that a^* lies between 0.2 and 0.3). Indeed, we see in Fig. 2 that the property $M = 0$ extends up to $a = a_a$, where a_a is located around $a \gtrsim 0.95$. The development of antiferromagnetic order cannot be easily observed by representing the value of the spins, as done in Fig. 3, since on a large scale one gets a uniform gray plot. On the other hand, it can be clearly seen by plotting the staggered spin σ_i instead of s_i, as it is done in Fig. 4. In this figure, local antiferromagnetic order results in black or white regions, and $|M| > 0$ corresponds to a majority of one of the two colors.

The very reason why antiferromagnetic order cannot establish up to such large fraction of antiferromagnetic interactions as $a = a_a$ is obviously related to the *ferromagnetic-always-wins* condition Eq. (11), as it is discussed in Appendix B. Beyond a_a the antiferromagnetic order sets in. This region will be discussed below (Sec. III A 3).

It is nowadays quite well established [30] that for the two-dimensional spin-glass model (corresponding to the choice $J_0 = 0$ in our notation) a zero temperature spin-glass phase exists, which, however, cannot be sustained at any finite temperature (i.e., $T_c = 0$ for this model). It is reasonable to think that a similar spin-glass order occurs in our model for $J_0 \neq 0$, provided we are in the paramagnetic region $a_f < a < a_a$. Although the dynamical results that will be presented below are clearly independent on any assumption regarding the nature of the ground state, we will later conform to the idea that a spin-glass phase exists to interpret the kinetic behaviors.

3. *Defective antiferromagnet ($a_a \leqslant a \leqslant 1$)*

In the region with $a > a_a$ there are very few and far apart ferromagnetic bonds. Due to the condition Eq. (11), the couples of spins attached to these bonds will be aligned. This represents a defect in the otherwise perfectly ordered antiferromagnetic state. Therefore, in this region the system is an antiferromagnet with a fraction $1 - a$ of isolated defects; the name *defective antiferromagnet* is due to this. One then has $m = 0$ and $M \neq 0$ in this region, as it can be seen in Fig. 2. We see from Fig. 4 that the local antiferromagnetic order parameter σ_i organizes in large regions as the critical point a_a is approached, similarly to what s_i does as the ferromagnetic transition at $a = a_f$ is narrowed. This suggests that the size ξ_a of such regions diverges at $a = a_a$, as it is sketched in Fig. 1, and that a continuous transition occurs.

B. Equilibrium states at finite temperature

Since we will consider the evolution of a system quenched to $T_f > 0$, it is worth discussing briefly the modifications to the above equilibrium picture at $T = 0$ introduced by a finite temperature. We must first keep in mind that the *ferromagnetic-always-wins* condition Eq. (11) implies

$$J_+ > |J_-|. \tag{12}$$

For instance, with our choices of the parameters we have $J_+ = 2.25$ and $|J_-| = 0.25$. In a standard system with a definite value J of the coupling constant it is $T_c \propto J$. Although in the present model J is not uniform, upon raising the temperature one expects that the antiferromagnetic ordering will be destroyed before the ferromagnetic one.

Let us now consider the region with $a < a_f$, where ferromagnetic order prevails. In this region the critical temperature is expected to drop from the Ising value $T_c(a = 0) \simeq 2.269 J_+ \simeq 5.105$, to $T_c(a = a_f) = 0$ (here and in the

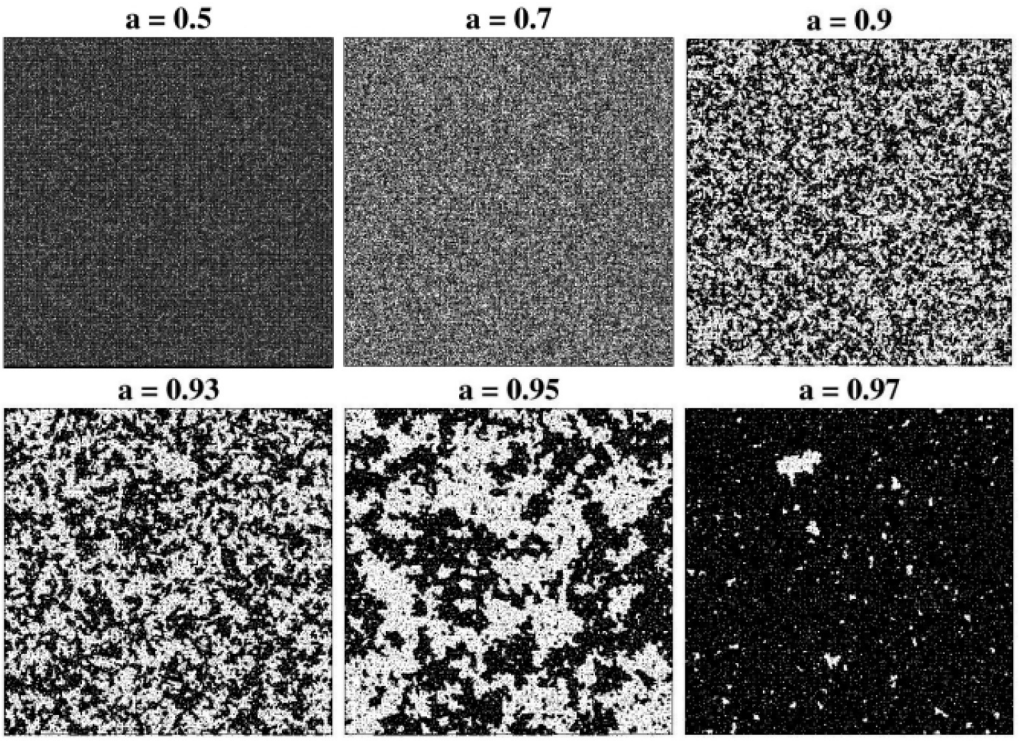

FIG. 4. Configurations of the ground state for a system of size $\mathcal{L} = 512$ for different values of a. We plot the staggered spin σ_i defined in Eq. (4). $\sigma_i = 1$ are plotted in black, $\sigma_i = -1$ in white.

following temperature is measured in units of the Boltzmann constant). Clearly, on the antiferromagnetic sector $a > a_a$ the corresponding critical temperature, which we will still denote with T_c, will drop from $T_c(a = 1) \simeq 2.269 J_- \simeq 0.567$ to $T_c(a_a) = 0$ upon decreasing a.

In the paramagnetic region, the spin-glass phase is expected to be destroyed by thermal fluctuations, no matter how small. Hence, $T_c = 0$ in this phase. However, as we will discuss further below, the existence of spin-glass order at $T = 0$ may strongly influence the dynamical properties at finite temperatures.

IV. KINETICS

The system is prepared in a fully disordered initial state with uncorrelated spins pointing randomly up or down, corresponding to an equilibrium configuration at $T = \infty$, and is then quenched at $t = 0$ to a low final temperature T_f. We evolve the model by means of single spin flips governed by the Glauber transition rates.

The main observable that we will consider is the inverse excess energy

$$L(t) = [E(t) - E_\infty]^{-1}, \tag{13}$$

where E_∞ is the energy of the equilibrium state at $T = T_f$. The latter has been obtained from the corresponding ground state by evolving it at $T = T_f$ until stationarity is achieved. For comparison, we have also found the equilibrium state directly by means of parallel tempering techniques. The values of E_∞ found with the two methods are consistent.

When the system has a simple ferromagnetic or antiferromagnetic order, as in clean or weakly disordered systems, the quantity in Eq. (13) can be straightforwardly identified with the size of the growing ordered regions. This is because in a coarsening process the interior of domains is in equilibrium and the excess energy is stored on the interface, so $E(t) - E(\infty)$ is proportional to their total length. This in turn is given by the length of a single domain's boundary [$\propto L(t)^{d-1}$] times the number of such domains ($\propto L^{-d}$), from which the relation Eq. (13) between the size $L(t)$ of domains and the excess energy is obtained.

Notice that the above identification of $L(t)$ with an ordering length relies on a number of assumptions: domains can be straightforwardly defined, they are equilibrated in their interior, and they are compact objects (i.e., they have an euclidean dimension, not a fractal one). While such assumptions are appropriate in a standard coarsening scenario, they cannot apply to the present model for any choice of a. Notably, the identification above almost surely fails in the paramagnetic region $a_f \leqslant a \leqslant a_a$. In these cases, $L(t)$ should prudentially be regarded simply as the inverse distance from the equilibrium energy.

Of course, the typical size of the growing structures can be measured—besides as in Eq. (13), also in many other ways. For example, in the ferromagnetic phase it can be easily extracted from the equal time spin correlation function $\langle s_i(t) s_{i+r}(t) \rangle$, where i and $i + r$ are two sites at distance r. Analogously, in a spin-glass phase one might use the equal time overlap correlator $\langle q_i(t) q_{i+r}(t) \rangle$, where

$$q_i = s_i(t) s_i^{GS} \tag{14}$$

is the overlap with the ground state. However, already in the ferromagnetic region, the result need not to be the same using different methods. Indeed, in a situation like the one of the ground state at $a = 0.4$ (upper right panel of Fig. 3), for instance, there are many islands with a finite extension. Then upon extracting a typical length from the correlation function at late times, one weights a lot the many small islands, which at long times are already equilibrated (hence coarsening is interrupted in their interiors) together with a comparatively smaller number of large islands. The latter are the only nonequilibrated regions within which phase-ordering is still active. Instead, using Eq. (13) one only focuses on those parts of the system where coarsening is still active, since inside the small equilibrated islands $E(t) \equiv E_\infty$ by definition. Hence, Eq. (13) is more suited to qualify how phase-ordering proceeds in the regions where it is still at work, while from the correlation function one obtains the average size of domains, irrespective of their state, weather in equilibrium or not. Since in this paper we are more interested to address the dynamical mechanisms driving the kinetics, we focus on the definition Eq. (13).

The difference between the value of L obtained from the definition Eq. (13) or from the spin-spin correlation function can be appreciated by looking to the inset of the lower panel of Fig. 5. Here, for a quench to $T_f = 0.75$, the typical length computed as in Eq. (13) is plotted for several values of a in the main picture, while the one obtained from the spin-spin correlation is reported in the inset (only for values of a in the ferromagnetic region). The latter determination grows much slowly than the former at $a = 0.4$, precisely because the ground states contains many small islands.

Let us now say a few words on the role of the final temperature T_f. Here we are interested in a situation where T_f is very small. This is because usually the kinetics of magnetic systems is more easily interpreted in this limit, and also because low temperatures guarantees $T_f < T_c(a)$—the situation we are interested in—in a wider range of a [see previous discussion about $T_c(a)$ in Sec. III B]. Setting T_f to very small values, however, has the undesirable consequence that the kinetics becomes so sluggish that no appreciable growth of $L(t)$ can be detected in the range of simulated times. In the following we will consider, out of many values T_f used in the simulations, the two choices $T_f = 0.4$ and $T_f = 0.75$, which were found to represent a good compromise between the two contrasting issues discussed above. Notice that both these temperatures are much below the critical temperature $T_c(a = 0)$ of the clean ferromagnet. On the other hand, while the former is smaller than that of the clean antiferromagnet $T_c(a = 1)$, the latter is above. Let us stress that, in any case, since $T_c(a_f \leqslant a \leqslant a_a) = 0$, for some values of a the quench is necessarily made above the critical temperature. We will comment further below on the implications of this.

A. Simulations

We now discuss the outcomes of our numerical simulations, splitting the presentation in Secs. IV A 1, IV A 2, and IV A 3 for quenches in the ferromagnetic, paramagnetic, and antiferromagnetic region, respectively. The general behavior of $L(t)$, in the whole range of values of a, is shown in Fig. 5, for

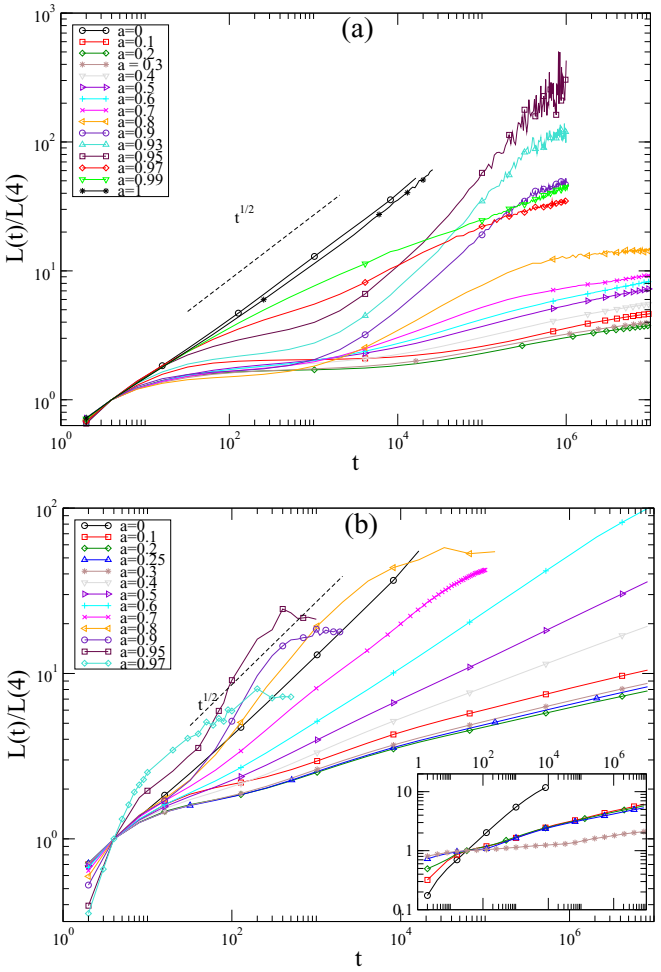

FIG. 5. $L(t)$ is plotted against time for a quench at $T_f = 0.4$ ((a), upper part) and at $T = 0.75$ ((b), lower part), for different values of a, in a double logarithmic plot. The black dashed line is the power-law $t^{1/2}$. The inset of the lower panel shows, for a quench to T_f and values of a restricted to the ferromagnetic region, the behavior of the characteristic length extracted from the spin correlation function (see text).

$T_f = 0.4$ and $T_f = 0.75$ (upper and lower panel, respectively). Notice that we plot $L(t)/L(t = 4)$ to better compare different curves.

As a general remark, we notice that at low temperature, such as for $T_f = 0.4$, $L(t)$ exhibit an oscillating behavior on top of the *neat* growth (namely the kind of growth that one would have if such oscillations were smoothed out in some way). This is quite commonly observed in disordered or inhomogeneous systems at low T_f [24,26,35] and is usually interpreted as due to the stop and go mechanism due to the pinning of interfaces. Indeed, an interface gets trapped in the configurations where it passes through weak bonds $J = J_-$. For instance, the smallest energetic barrier ΔE encountered by a piece of interface occurs when it has to move from a position where it intersects a single antiferromagnetic bond to one where it crosses only ferromagnetic ones. This situation is likely to be observed when there are few antiferromagnetic bonds around, namely for small a. In this case, $\Delta E = J_+ - J_- = 2K$. The associated Arrhenius time to escape the pinned state is $\tau \simeq$

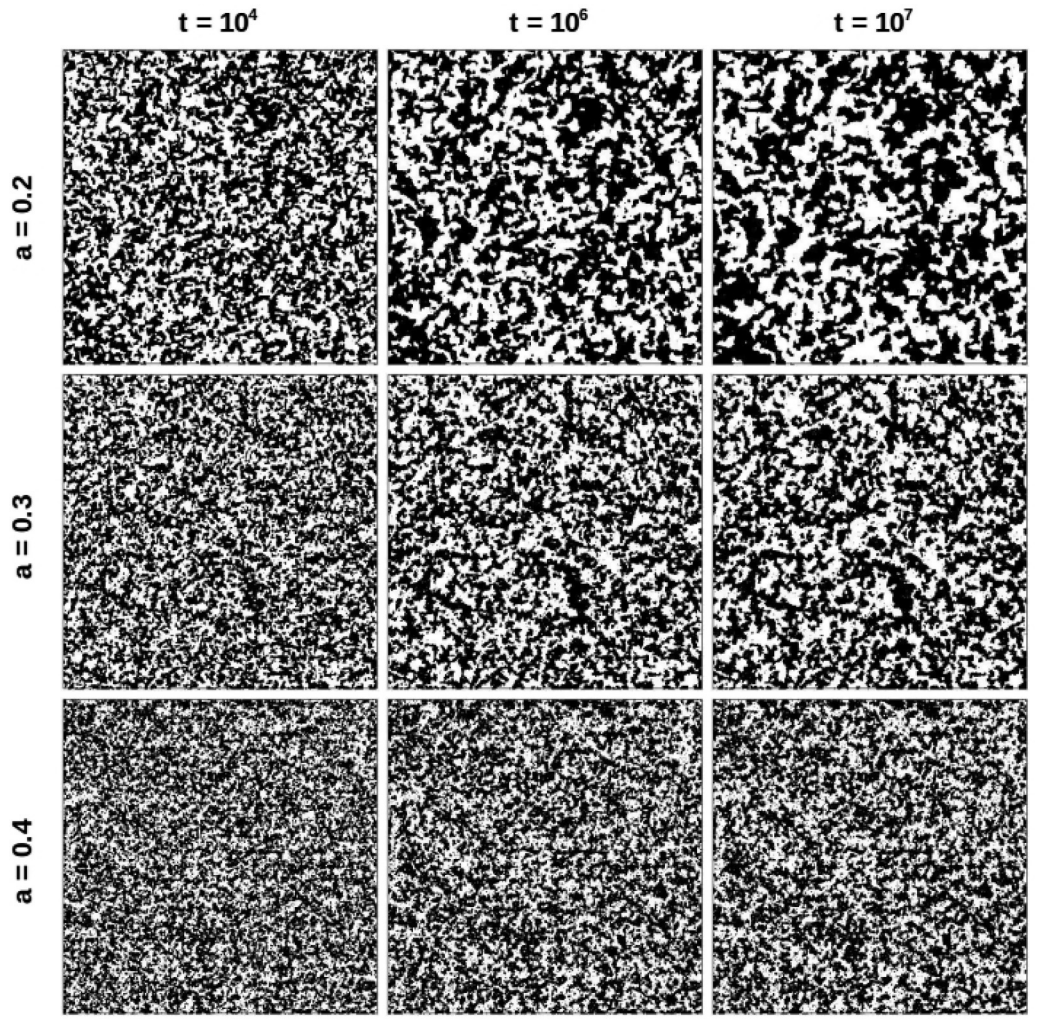

FIG. 6. Configurations of spins for a system of size $\mathcal{L} = 512$ quenched to $T_f = 0.4$ for $a = 0.2$ (upper row), $a = 0.3$ (central row), and $a = 0.4$ (lower raw). First columns report configurations at $t = 10^4$, the central one at $t = 10^6$, and the left one at $t = 10^7$. Spins up are plotted in black, spins down in white.

$\exp[-\Delta E/(K_B T)$. With the parameters of our simulations one has $\tau \simeq 518$ for $T_f = 0.4$ and $\tau \simeq 28$ for $T_f = 0.75$. One sees in Fig. 5 that, for $T_f = 0.4$, this value is very well compatible with the time where $L(t)$, after becoming very slow, starts growing faster again (a rough agreement is found also for $T_f = 0.75$, although in this case the oscillatory phenomenon is only hinted).

Oscillations shadow the genuine growth law, and it is therefore almost impossible to come up with any quantitative statement about the neat growth, e.g., if it consistent with a power law or a logarithm or else. As the final temperature is raised, the stop and go mechanism, although still present, is less coherent, and the oscillations are smeared out. This is observed at $T_f = 0.75$. Moreover, the speed of ordering increases upon raising T_f, as it is expected in the presence of activated dynamics.

1. *Ferromagnetic region* $0 \leqslant a \leqslant a_f$

Snapshots of the system's configuration at different times after a quench to $T_f = 0.4$, and for three different choices of a, are shown in Fig. 6. For any value of a one clearly observes a coarsening phenomenon with domains of the two phases growing in a self-similar way in time. Upon increasing a, domains look more jagged and indented, presumably due to the nearing of the critical point at $a = a_f$ where, as usual in second-order phase-transitions, a fractal structure is expected to appear.

Concerning the size $L(t)$ of such growing structures (Fig. 5), starting from the pure case with $a = 0$ (black curve with circles), where the expected behavior $L(t) \propto t^{1/2}$ is well represented, the growth law slows down upon rising a, but this occurs only up to a certain value a, which we interpret as $a = a^*$ and is located around $a = 0.2$. Upon increasing a beyond a^*, the phase-ordering process speeds up again, up to a_f. This is very well observed both for $T_f = 0.4$ and $T_f = 0.75$. The value of a^*, at these two temperatures, is comparable, as it is expected since this quantity was previously defined in a purely geometrical way.

In previous papers [24–26], we have shown that the growth rate $r = dL/dt$ of $L(t)$, namely the speed of growth, varies in a nontrivial way as the amount of disorder in a ferromagnetic model is changed. Specifically, in a system where a fraction d of lattice sites or bonds is randomly removed, the speed of growth is at its maximum for the pure system at $d = 0$. As d

is increased, disorder pins the interfaces and r decreases. The larger is d, the larger is the pinning effect, and the smaller is r. However, this is only true for moderate values of d, namely for $d \leqslant d^*$. Raising d above d^* one observes that r starts to increase again up to the largest possible value of d, namely $d = d_p$, where $d_p = 1 - p_c$, p_c being the critical threshold of random percolation. For $d > d_p$ the network where the spins live becomes disconnected and the ferromagnetic properties are lost. It turns out that d^* is roughly in the middle between $d = 0$ and $d = d_p$. The interpretation of this non monotonic behavior of r, given in Refs. [24–26], is the following: besides the pure case, where the speed of growth is at its maximum, the other network where $L(t)$ grows relatively fast (but slower than in the pure case) is the percolation fractal at $d = d_p$. This is argued to be due to the critical properties of such network, which in turn are responsible of the fact that, right at $d = d_p$, the transition temperature of the model $T_c(d = d_p)$ vanishes. Indeed the fractal properties of the structure at $d = d_p$ soften the energetic barriers that pin the interfaces, making in this way the evolution faster. Since there are a global and a relative maximum of r at $d = 0$ and $d = d_p$, respectively, there must be a minimum somewhere in between. This value is d^*. This explains why r is a non monotonic function of a.

Also in the present model the geometric properties of the system are such that there is a point, namely $a = a_f$, where $T_c(a = a_f)$ vanishes (actually the same occurs at $a = a_a$, where an analogous discussion is expected to hold). Therefore, upon repeating the argument above (with the obvious replacements $d \to a$ and $d_p \to a_f$), one could expect r to be at its global maximum at $a = 0$, to decreases as a increases up to a value a^* located in between $a = 0$ and $a = a_f$, and then to rise again up to $a = a_f$. This is precisely what we see in Fig. 5. The nonmonotonic dependence of the speed of growth on disorder, therefore, qualifies as a rather general property of ferromagnetic systems and a common interpretation for different models can be provided.

Let us also mention that in Refs. [24–26] not only the nonmonotonic behavior discussed insofar was shown, but a quantitative conjecture was put forth: the asymptotic growth law should be of the logarithmic type in the whole disordered region $0 < d < d_p$, while it ought to be algebraic $L(t) \propto t^{1/z}$ both in the clean case $d = 0$ (with $z = 2$) and at $d = d_p$ (with $z > 2$ and T_f-dependent). For d close to $d = 0$ (or to d_p) the logarithmic growth is shadowed preasymptotically by the algebraic behavior induced by the proximity of the clean point $d = 0$ (or the percolative one $d = d_p$). Notice that, in some cases, algebraic preasymptotic behaviors have been shown to leave room to a truly logarithmic growth only after huge times, a notable example being the random bond Ising model with a continuous distribution of ferromagnetic coupling constants [32]. This originated a lot of contradicting conclusions in the past.

If a mechanism akin to the one discussed above is at work also in the present model one would expect an asymptotic logarithmic behavior (after a—possibly slow—crossover) for any $0 < a < a_f$, and a power-law behavior of $L(t)$ right at $a = a_f$. While nothing can be said, as discussed above, for quenches to $T_f = 0.4$ due to the oscillating nature of the curves, this conjecture can be tested to some extent in the data for $T_f = 0.75$. This can be done by computing the effective exponent $z_{\rm eff}$, defined as

$$\frac{1}{z_{\rm eff}(t)} = \frac{d[\ln L(t)]}{d[\ln t]}. \tag{15}$$

This quantity is plotted in Fig. 7. For $a = 0$ it approaches the expected asymptotic value $1/z_{\rm eff} = 1/2$ starting from relatively early times $t \simeq 10^3$. As a is progressively increased from $a = 0$ to $a = 0.4 \simeq a_f$, the effective exponent becomes, for a given late time, initially smaller (in the range $0 \leqslant a \leqslant a^* \simeq 0.2$) and then rises again (moving a in the range $a^* \leqslant a \leqslant a_f$).

Concerning the time evolution of $1/z_{\rm eff}$ our data clearly show that it keeps steadily decreasing in the late regime with $t \gtrsim 10^4$ for all the values of a in the range $0 < a \leqslant 0.3$. The decrease is rather slow but reliable. This implies that the growth law of $L(t)$ is slower than algebraic. Although the curves for $L(t)$ span a vertical range that is too limited to allow a precise determination of such law (furthermore, a weak oscillation is present up to times of order 10^4), we can at least conclude that the decrease of $1/z_{\rm eff}$ agrees with the expectation of a logarithmic behavior. Data for $a = 0.4 \simeq a_f$, on the other hand, are quite well consistent with a constant behavior of $1/z_{\rm eff} \simeq 0.19$ at late times, and this also agrees with the conjecture discussed above. Finally, the effective exponent looks rather constant also for $a = 0.37$. This can be ascribed to the preasymptotic algebraic behavior induced by the proximity of the percolation point $a = a_f$. We expect, therefore, that a decrease of $1/z_{\rm eff}$ would be observed also for $a = 0.37$ if sufficiently long times could be accessed in the simulations.

Notice that an algebraic law is also observed in the whole paramagnetic region, an interpretation of which will be provided in the next section. Therefore, the different asymptotic behavior—i.e., algebraic versus logarithm—observed at $a = a_f$ with respect to the rest of the ferromagnetic region $0 < a < a_f$ can also be interpreted upon thinking a_f as the lower limit of the paramagnetic region where algebraic behaviors are observed. We will comment further on this point below.

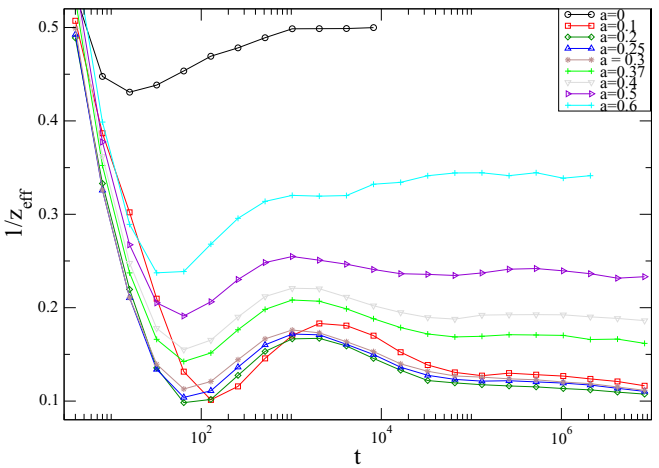

FIG. 7. The effective exponent $1/z_{\rm eff}(t)$ is plotted against time for a quench at $T = 0.75$, for different values of a, in a double logarithmic plot.

2. *Paramagnetic region $a_f < a < a_a$*

In two-dimensional spin glasses (corresponding to $J_0 = 0$ in our model), it was shown [36–38] that the existence of a spin-glass phase at $T = 0$ rules the kinetic in a long-lasting preasymptotic regime. The situation is akin to what was observed in the clean Ising model at the lower critical dimension $d_L = 1$ after a quench to a finite but low enough temperature. In this case, it can be shown [39,40] that the kinetics proceeds as in a quench to $T_f = 0$ until $L(t) \simeq \xi$, where $\xi = e^{2J_0/T_f}$ is the equilibrium coherence length. Since this quantity is huge, the preasymptotic regime where nonequilibrium kinetics is observed extends to very long times at low T_f. Afterwards, aging is interrupted and the system equilibrates. In the $d = 2$ spin glass, it is found that as long as the preasymptotic stage is considered, a growing length can be identified which exhibits an algebraic behavior [37].

In the present model, assuming that a kind of spin-glass order is developed at $T_f = 0$ in the paramagnetic region $a_f < a < a_a$, we expect to observe a similar phenomenon. This can be already appreciated at a qualitative level in Fig. 8. In this set of figures we plot the local overlap [Eq. (14)] between the actual dynamical spin configurations and the ground state, for different times after a quench to $T_f = 0.4$, and for three different choices of a. Interestingly, also in this paramagnetic phase, for any value of a, one clearly observes a coarsening phenomenon with domains of the two phases growing in a self-similar way in time, although quite slowly. This agrees with what was observed in Ref. [37]. Moreover, there is no signal of equilibration at any time, nor does the growth seem to be interrupted. As a further comment, we notice that configurations appear much more rugged for larger values of a.

The study of the approach to equilibrium can be made more quantitative by inspection of Fig. 5, where $L(t)$ for the various cases is plotted. Here one sees that, as already anticipated, data for $T_f = 0.75$ are consistent with an algebraic growth $L(t) \propto t^{1/z}$, with an a-dependent exponent, in agreement with Ref. [37]. Data for $a \geqslant 0.7$ clearly bend downwards at late times, indicating that equilibration is starting to be achieved. The algebraic increase of $L(t)$ is further confirmed by inspection of the effective exponent $z_{\rm eff}$ in Fig. 7. This quantity stays basically constant, besides some noisy behavior,

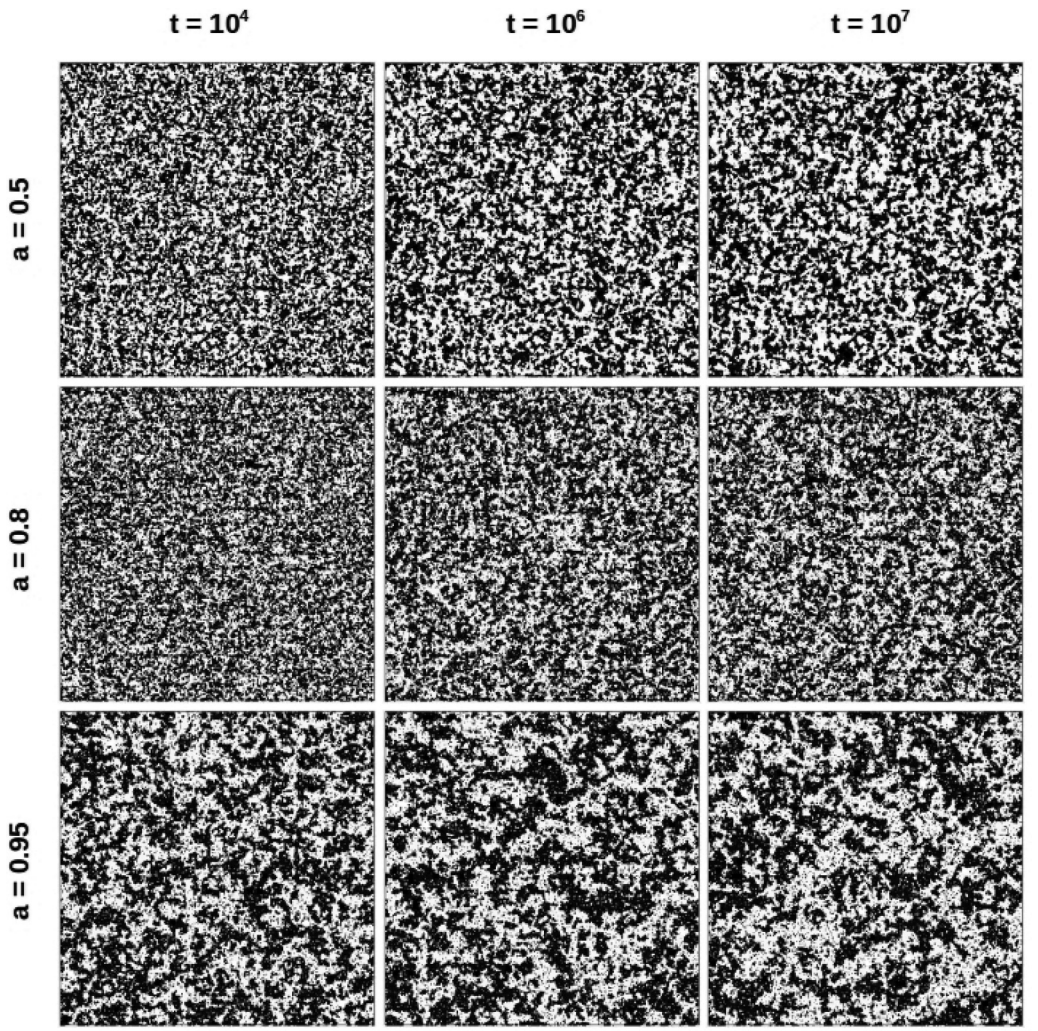

FIG. 8. Configurations of the overlap, as defined in Eq. (14), for a system of size $\mathcal{L} = 512$ quenched to $T_f = 0.4$ for $a = 0.5$ (upper row), $a = 0.8$ (central row), and $a = 0.95$ (lower raw). First columns report configurations at $t = 10^4$, the central one at $t = 10^6$, and the left one at $t = 10^7$. Positive overlaps are plotted in black, negative ones in white.

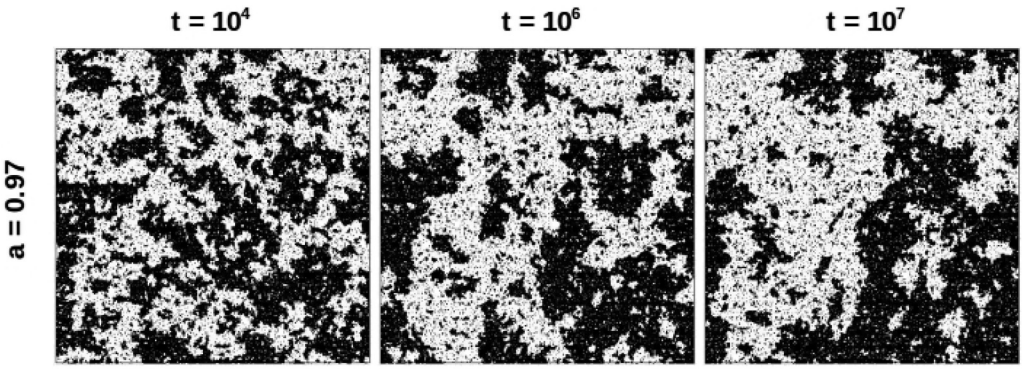

FIG. 9. Configurations of the staggered spin, as defined in Eq. (4), for a system of size $\mathcal{L} = 512$ quenched to $T_f = 0.4$ for $a = 0.97$ for times $t = 10^4$, $t = 10^6$, $t = 10^7$. Positive σ_i's are plotted in black, negative ones in white.

in the late time regime $t \gtrsim 10^3$–10^4. Notice also that $1/z_{\rm eff}$ raises as a is increased. This can be ascribed, at least partly, to the fact that the largest barriers encountered are associated to the positive couplings [since condition Eq. (12) holds], and the number of the latter is reduced upon increasing a.

A power-law for $L(t)$ in this paramagnetic region, as opposed to the logarithmic one in most disordered ferromagnetic models, including the one at hand for $0 < a < a_f$, can perhaps be read into the different structure of the low-energy states. For a ferromagnet there are two degenerate ground states separated by an energetic barrier. A common picture of a frustrated system is, instead, one with many quasiequivalent low-energy states. Taking advantage of entropic effects, the system can move among these states lowering in this way the free-energy barriers. This could speed up the evolution from logarithmic to algebraic.

3. *Region with antiferromagnetic order* $a \geqslant a_a$

In Fig. 9 we plot the configurations of the staggered spin σ_i—see Eq. (4)—at different times, which clearly show the coarsening phenomenon. In this region with antiferromagnetic order we expect a situation mirroring the one discussed in the ferromagnetic region, with the obvious correspondences $a = 0 \leftrightarrow a = 1$ and $a = a_f \leftrightarrow a = a_a$. Since in this case $T_c(a = 1) \simeq 0.567$, as already discussed, there is no room left to observe coarsening for $T_f = 0.75$ for any value of $a < 1$ (indeed for $T_f = 0.75$—in the lower panel of Fig. 5—$L(t)$ flattens very soon, saturating to the equilibrium value). Let us then focus only on the upper panel of Fig. 5, where data for $T_f = 0.4$ are presented. Here one observes the nonmonotonic behavior of the speed of ordering r already discussed when considering the ferromagnetic phase. Upon decreasing a from the clean value $a = 1$, the kinetics quickly becomes much slower in going to $a = 0.97$, and then r increases again until the border of the paramagnetic phase is touched at $a = a_a \gtrsim 0.95$.

V. CONCLUSIONS

In this paper, we have studied numerically a two-dimensional random bond Ising model where a fraction $1 - a$ of coupling constants is positive $J = J_+ > 0$ and the remaining ones are negative, $J = J_- < 0$. The choice of J_+ and J_- has been made according to a *ferromagnetic-always-wins* condition, which strongly favors ferromagnetic ordering. We have classified the low-temperature equilibrium states according to the values taken by the magnetization m and the staggered magnetization M. We have shown the existence of a ferromagnetic and an antiferromagnetic phase for $a < a_f$ and $a > a_a$. In between, for $a_f < a < a_a$, there is a paramagnetic phase at any temperature T, presumably with spin-glass order at $T = 0$.

The main focus of the paper has been on the off-equilibrium evolution of the model after a quench from an infinite temperature disordered state to low temperatures. In the ferromagnetic and antiferromagnetic phases the process amounts to the much studied coarsening phenomenon in the presence of quenched disorder, which is characterized by the everlasting increase of the typical domains' size $L(t)$.

Also in the present model, we find that the speed of the nonequilibrium evolution varies in a nonmonotonic way as the amount of disorder a is increased, similar to what was observed in other disordered ferromagnets [24–26]. Specifically, there exists a value $a^* \sim 0.2$ where the kinetics is slower than for any other value of a. We have also been able to show that the growth law of $L(t)$ is slower than algebraic, i.e., of a logarithmic type, in the whole ferromagnetic (and antiferromagnetic) region $0 < a < a_f$ (or $a_a < a < 1$). Interestingly enough, this is true both for $0 \leqslant a \leqslant a^*$ and for $a^* \leqslant a < a_f$, irrespective of the fact that the structure of the ferromagnetic state is different in these two sectors, because the system is a perfect ferromagnet (i.e., $m^2 = 1$ at $T = 0$) in the former range while it contains a number of defects (antiferromagnetic inclusions) in the latter (so that $m^2 < 1$ at $T = 0$).

Similar considerations can be made in the paramagnetic region. Here we find that $L(t)$, the inverse excess energy, grows algebraically in the whole phase, irrespective of the fact that the geometrical properties of the bond network greatly change as a is varied in $[a_f, a_a]$.

These results seem to indicate that $L(t)$ is able to discern between systems with a ferromagnetic phase extending below a finite critical temperature $T_c > 0$ from the others. In the former $L(t)$ grows in a logarithmic way, whereas a power-law is observed otherwise. The results of this paper show that this property, which was already found in models of disordered magnets without frustration [24–26], extends its validity to the realm of frustrated systems, pointing toward a general robustness.

ACKNOWLEDGMENTS

We thank Hamid Khoshbakht for discussions and significant help in the determination of the ground states. We thank Federico Ricci-Tersenghi for useful discussions. F.C. acknowledges financial support by MIUR Grant No. PRIN 2015K7KK8L.

APPENDIX A: SUPPRESSION OF FERROMAGNETIC ORDER FOR $a \gtrsim a_f$

For $a \gtrsim a_f$, the amount of negative bonds is sufficient to spoil the ferromagnetic order. This may happen, for instance, when the spanning sea of ferromagnetic bonds have a thin part, like the horizontal path within the two dashed orange lines in the left panel of the schematic Fig. 10, along which spins cannot keep the same orientation without increasing the total energy. In the situation sketched, it is easy to check that the represented configuration minimizes the energy.

This picture has been presented to easily grasp the properties of the ground state, but it is not appropriate to describe the situation with $a < a_p$. Indeed, for such values of a there cannot be a spanning path of antiferromagnetic bonds, while it is present in Fig. 10 (along the dashed orange lines). However, one can easily check that the ground state does not change if a certain fraction $f \leqslant 1/z$ (in this case $f \leqslant 1/4$) of the antiferromagnetic bonds crossing the dashed orange lines are turned into ferromagnetic ones. In this new situation there are no spanning clusters of antiferromagnetic bonds, but the ground state is still split into four pieces with discording magnetization.

A computation of a_f looks very difficult, since this amount to evaluate the smallest probability a such that a spanning object formed by a fraction $1 - f$ of antiferromagnetic bonds exists. An (admittedly very rough) estimation is the following: We know that at $a = a_p$ a spanning path of antiferromagnetic bonds exists. If the probability is decreased to $(1 - f)a_p$, a fraction f of such antiferromagnetic bonds will be converted to ferromagnetic ones. This provides $a_f \simeq (1 - f)a_p$. In our two-dimensional case this yields $a_f \simeq 3/8 = 0.375$, to be compared with the observed value $a_f \gtrsim 0.4$.

APPENDIX B: SUPPRESSION OF ANTIFERROMAGNETIC ORDER FOR $a \lesssim a_a$

The reason why antiferromagnetic order cannot establish up to fractions of negative bonds as large as $a_a \simeq 0.95$ can be easily understood by looking at the schematic ground state situation of the right panel of Fig. 10. In this picture it is seen that also a small amount of ferromagnetic bonds can induce an interface (of the antiferromagnetic type—marked by a dashed magenta line) in the system. Indeed, it is easy to check that, due to the condition Eq. (11), the situation where such an interface is removed corresponds to an higher energy. Because of the interface, the system is split in regions with mismatched staggered magnetization and hence $M = 0$. Clearly, the formation of the interface in the right panel of Fig. 10 becomes energetically unfavorable if the density of ferromagnetic bonds (basically the distance between blue bonds in Fig. 10) becomes too small. A rough estimation of the value of a where this occurs is the following. The average distance between ferromagnetic bonds is λ_f. Along an interface, such as the one plotted in Fig. 10, there is a ferromagnetic bond of strength J_+ every λ_f antiferromagnetic ones (of strength J_-). Hence, the interface cannot be sustained if $\lambda_f |J_-| > J_+$, namely for

$$(1 - a)^{-d} > \frac{J_+}{|J_-|}, \tag{B1}$$

where we have used Eq. (9). With the choice $J_0 = 1$, $K = 1.25$ adopted in our simulations, this would predict the interface instability at $a = a_a = 0.7$. This is only a lower bound

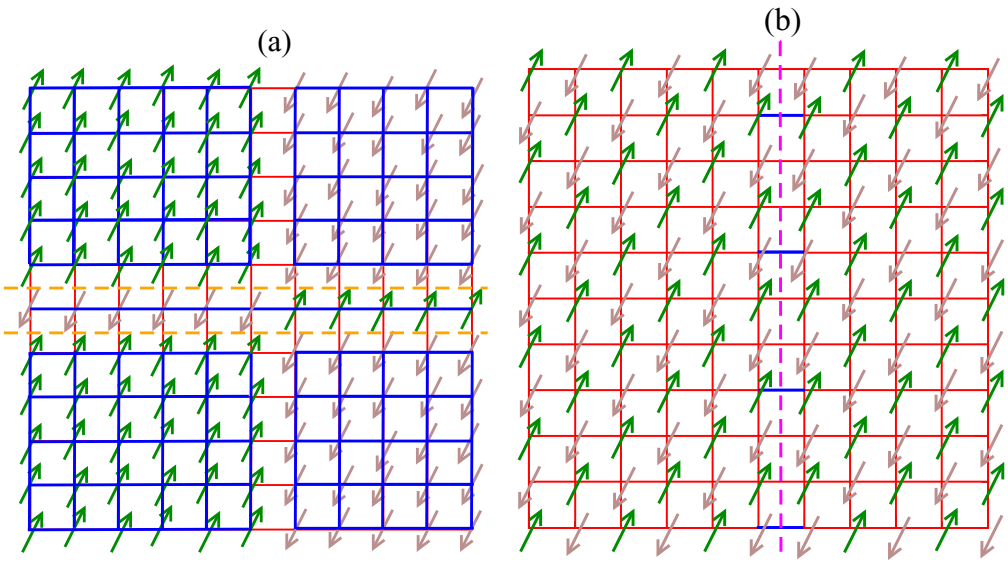

FIG. 10. Schematic representations of the ground states of the system in the regions $a_f < a < a_p$ ((a), left part) and $a_p < a < a_a$ ((b), right part). Antiferromagnetic and ferromagnetic bonds are drawn in red and blue, respectively. Spins up and down are colored in green and brown, respectively. In the left panel, the two dashed orange lines indicate paths of antiferromagnetic bonds. In the right panel, the dashed magenta line is an interface in the antiferromagnetic order.

to the value of a_a, since it is clear that besides having condition Eq. (B1) obeyed, other conditions must apply. For instance, an antiferromagnetic bond must be guaranteed next to the ferromagnetic ones. Indeed, we see in Fig. 2 that the paramagnetic phase extends much beyond $a = 0.7$, at least up to $a_a \sim 0.95$.

[1] A. J. Bray, Adv. Phys. **43**, 357 (1994); *Kinetics of Phase Transitions*, edited by S. Puri and V. Wadhawan (CRC Press, Boca Raton, 2009).
[2] F. Corberi, C. R. Phys. **16**, 332 (2015).
[3] H. Ikeda, Y. Endoh, and S. Itoh, Phys. Rev. Lett. **64**, 1266 (1990).
[4] A. G. Schins, A. F. M. Arts, and H. W. d. Wijn, Phys. Rev. Lett. **70**, 2340 (1993).
[5] D. K. Shenoy, J. V. Selinger, K. A. Grüneberg, J. Naciri, and R. Shashidhar, Phys. Rev. Lett. **82**, 1716 (1999).
[6] V. Likodimos, M. Labardi, X. K. Orlik, L. Pardi, M. Allegrini, S. Emonin, and O. Marti, Phys. Rev. B **63**, 064104 (2001); V. Likodimos, M. Labardi, and M. Allegrini, *ibid.* **61**, 14440 (2000).
[7] Z. W. Lai, G. F. Mazenko, and O. T. Valls, Phys. Rev. B **37**, 9481 (1988).
[8] G. S. Grest and D. J. Srolovitz, Phys. Rev. B **32**, 3014 (1985).
[9] M. Rao and A. Chakrabarti, Phys. Rev. E **48**, R25(R) (1993).
[10] E. Lippiello, A. Mukherjee, S. Puri, and M. Zannetti, Europhys. Lett. **90**, 46006 (2010).
[11] D. S. Fisher, P. Le Doussal, and C. Monthus, Phys. Rev. E **64**, 066107 (2001); Phys. Rev. Lett. **80**, 3539 (1998).
[12] F. Corberi, A. de Candia, E. Lippiello, and M. Zannetti, Phys. Rev. E **65**, 046114 (2002).
[13] M. Rao and A. Chakrabarti, Phys. Rev. Lett. **71**, 3501 (1993); C. Aron, C. Chamon, L. F. Cugliandolo, and M. Picco, J. Stat. Mech. (2008) P05016.
[14] F. Corberi, E. Lippiello, A. Mukherjee, S. Puri, and M. Zannetti, Phys. Rev. E **85**, 021141 (2012).
[15] S. Puri and N. Parekh, J. Phys. A **26**, 2777 (1993); E. Oguz, A. Chakrabarti, R. Toral, and J. D. Gunton, Phys. Rev. B **42**, 704 (1990); E. Oguz, J. Phys. A **27**, 2985 (1994).
[16] S. Sinha and P. K. Mandal, Phys. Rev. E **87**, 022121 (2013); P. K. Mandal and S. Sinha, *ibid.* **89**, 042144 (2014).
[17] S. Puri, D. Chowdhury, and N. Parekh, J. Phys. A **24**, L1087 (1991); S. Puri and N. Parekh, *ibid.* **25**, 4127 (1992); A. J. Bray and K. Humayun, *ibid.* **24**, L1185 (1991); B. Biswal, S. Puri, and D. Chowdhury, Physica A **229**, 72 (1996).
[18] R. Paul, G. Schehr, and H. Rieger, Phys. Rev. E **75**, 030104(R) (2007).
[19] H. Park and M. Pleimling, Phys. Rev. B **82**, 144406 (2010).
[20] D. A. Huse and C. L. Henley, Phys. Rev. Lett. **54**, 2708 (1985).
[21] J. Villain, Phys. Rev. Lett. **52**, 1543 (1984).
[22] R. Paul, S. Puri, and H. Rieger, Europhys. Lett. **68**, 881 (2004); Phys. Rev. E **71**, 061109 (2005).
[23] M. Henkel and M. Pleimling, Europhys. Lett. **76**, 561 (2006); Phys. Rev. B **78**, 224419 (2008); J. H. Oh and D.-I. Choi, *ibid.* **33**, 3448 (1986).
[24] F. Corberi, M. Zannetti, E. Lippiello, R. Burioni, and A. Vezzani, Phys. Rev. E **91**, 062122 (2015).
[25] F. Corberi, E. Lippiello, A. Mukherjee, S. Puri, and M. Zannetti, Phys. Rev. E **88**, 042129 (2013).
[26] F. Corberi, E. Lippiello, and M. Zannetti, J. Stat. Mech. (2015) P10001.
[27] F. Corberi, E. Lippiello, and M. Zannetti, Europhys. Lett. **116**, 10006 (2016).
[28] F. Corberi, L. F. Cugliandolo, F. Insalata, and M. Picco, Phys. Rev. E **95**, 022101 (2017).
[29] F. Corberi, L. F. Cugliandolo, and H. Yoshino, in *Dynamical Heterogeneities in Glasses, Colloids, and Granular Media*, edited by L. Berthier, G. Biroli, J.-P. Bouchaud, L. Cipelletti, and W. V. Saarloos (Oxford University Press, Oxford, 2011).
[30] C. Amoruso, E. Marinari, O. C. Martin, and A. Pagnani, Phys. Rev. Lett. **91**, 087201 (2003); T. Jorg, J. Lukic, E. Marinari, and O. C. Martin, *ibid.* **96**, 237205 (2006).
[31] M. Mézard, G. Parisi, and M. A. Virasoro, *Spin Glass Theory and Beyond* (World Scientific, Singapore, 1987).
[32] F. Corberi, E. Lippiello, A. Mukherjee, S. Puri, and M. Zannetti, J. Stat. Mech. (2011) P03016.
[33] H. Khoshbakht and M. Weigel (unpublished).
[34] C. K. Thomas and A. A. Middleton, Phys. Rev. B **76**, 220406 (2007).
[35] R. Burioni, D. Cassi, F. Corberi, and A. Vezzani, Phys. Rev. E **75**, 011113 (2007); R. Burioni, F. Corberi, and A. Vezzani, J. Stat. Mech. (2009) P02040; Phys. Rev. E **87**, 032160 (2013).
[36] H. Rieger, B. Steckemetz, and M. Schreckenberg, Europhys. Lett. **27**, 485 (1994); J. Kisker, L. Santen, M. Schreckenberg, and H. Rieger, Phys. Rev. B **53**, 6418 (1996); S. Franz, V. Lecomte, and R. Mulet, Phys. Rev. E **68**, 066128 (2003).
[37] H. Rieger, G. Schehr, and R. Paul, Prog. Theor. Phys. Suppl. **157**, 111 (2005).
[38] C. Chamon, F. Corberi, and L. F. Cugliandolo, J. Stat. Mech. (2011) P08015.
[39] R. J. Glauber, J. Math. Phys. **4**, 294 (1963).
[40] F. Corberi, E. Lippiello, and M. Zannetti, Eur. Phys. J. B **24**, 359 (2001).